Project Title: Low-cost, reliable soft arm for automated tree fruit operations

Report Type: Final Project Report

Primary PI: Ming Luo
Organization: Washington State University
Telephone: 509-335-4034
Email: ming.luo@wsu.edu
Address: 355 NE Spokane St
Address 2:
City/State/Zip: Pullman/WA/99163

Co-PI 2: Manoj Karkee
Organization: Washington State University
Telephone: 509-786-9208
Email: manoj.karkee@wsu.edu
Address: 24106 N. Bunn Road
Address 2:
City/State/Zip: Prosser/WA/99350

CO-PI 3: Matthew David Whiting
Organization: Washington State University
Telephone: 509-786-9260
Email: mdwhiting@wsu.edu
Address: 24106 N. Bunn Road
Address 2:
City/State/Zip: Prosser/WA/99350

Cooperators: Dave Allan, Allan Brothers Fruits; Tim Welsh, Columbia Orchard Management, Inc.; FFRobotics, Israel

Project Duration: 1-Year

Total Project Request for Year 1 Funding: $ 122,476

Other related/associated funding sources: Awarded,

Funding Duration: 2022
Amount: $50,000 + 1 year research assistantship
Agency Name: WSU Multi-disciplinary Grant
Notes: Title: Universal Robotic Solution for Future Tree Fruit Orchards.
This funding supports us to develop large grant (USDA SCRI/SCMP) which includes the soft grow manipulator.

WTFRC Collaborative Costs: None

Budget 1
Primary PI: Ming Luo
Organization Name:
Contract Administrator: Ian Leibbrandt
Telephone:
Contract administrator email address: ian.leibbrandt@wsu.edu
Station Manager/Supervisor:
Station manager/supervisor email address:

Item	2022
Salaries	$31,615.00
Benefits	$5,618.00
Wages	$13,800.00
Benefits	$243.00
RCA Room Rental	
Shipping	
Supplies	$5,000.00
Travel	$3,000.00
Plot Fees	
Miscellaneous	
Total	$59,276.00

Footnotes:

If project duration is only 1 year, delete Year 2 and Year 3 columns.

(*Complete the following budget tables if funding is split between organizations,* ***otherwise delete*** *extra tables.)*

Budget 2
Co PI 2: Manoj Karkee
Organization Name:
Contract Administrator: Samantha Bridger
Telephone:
Contract administrator email address: prosser.grants@wsu.edu
Station Manager/Supervisor:
Station manager/supervisor email address:

Item	2022
Salaries	$21,393.00
Benefits	$2,696.00
Wages	$13,800.00
Benefits	$243.00
RCA Room Rental	
Shipping	
Supplies	
Travel	$5,000.00
Plot Fees	
Miscellaneous	
Total	$43,132.00

Footnotes:

If project duration is only 1 year, delete Year 2 and Year 3 columns.

Budget 3
Co-PI 3: Matthew Whiting
Organization Name:
Contract Administrator: Samantha Bridger
Telephone:
Contract administrator email address: prosser.grants@wsu.edu
Station Manager/Supervisor:
Station manager/supervisor email address:
Email Address:

Item	2022
Salaries	16045
Benefits	2022
Wages	
Benefits	
RCA Room Rental	
Shipping	
Supplies	2000
Travel	
Plot Fees	
Miscellaneous	
Total	$20,067.00

Footnotes:

Recap original objectives and significant findings

Objective#1: Design, fabricate, test, and optimize a growing arm/manipulator for orchard operations (Luo – Lead, Karkee – Co Lead;)

Overview in the proposal: To perform various field operations in tree fruit production, our soft growing manipulator will have the following mechanical features: 1) 7 ft radius workspace - the proposed manipulator length (7 ft) is expected to cover the entire tree height (~14ft) when installed on a ground platform that is approximately half of the tree height. 2) Free movement in 3D space with up to 3 lbs payload (which is sufficient to carry most of the end-effectors such as a fruit picker or an electric scissors for pruning) - Our proposed manipulator must overcome gravity to grow, retract, and steer to reach any target within its workspace. 3) Ability to maneuver freely inside most tree canopies under 14 ft height: The diameter of our proposed manipulator and updated design of end-effector adaptor/mount allows the manipulator to pass through narrow spaces between branches.

Our current achievement:

Soft growing manipulator:

- *Length:* can extend 4 ft (We found 4 ft is enough length to achieve apple harvesting according to the current modern orchard's tree architecture and commercial robotic platforms.
- *Speed:* Growing speed, manipulator displays 0.7 ft/s growing speed at 7 psi. We have observed that higher internal pressure results in dramatically faster extension speed. Based on our analytical calculations, we can achieve an extension/growing speed of 1.7 ft/s. There are two ways to increase the speed. One is to increase the pressure, however, due to safety issues in the lab, higher pressure cannot be reliably tested. The second one is to increase the air flow rate. We are working on the latter approach to increase the size of the outlet of the container, and we will update the results during our presentation.
- *Payload:* 2 lbs payload around 9 psi pressure input. The current payload of the end-effector including the tip mount and the soft robotic gripper is around 1 lbs, so there is sufficient payload to carry an apple under 1 lbs. The payload can be increased by the increase of the pressure input.
- *Workspace:* One ZED2 camera is able to detect around 6ft * 6ft range within 3 ft depth. Our robot's workspace has a spherical sector shape with a radius of 4 ft and 60 degrees of actuation in the 2D plane.
- Reliability: The maximum input pressure of our fabric material's sealing is around 18 psi, and 9 psi is our operation pressure since it has enough payload. In addition, we install the pressure relief valve to reduce the risk of pressure overloading. For future work, we are collaborating with Dr. Liu, a polymeric fabric expert at WSU, to improve the sealing technique used to create the fabric arms.
- R&D cost: The current prototyping cost of a single robot manipulator is eight times less than a single commercially available rigid manipulator. The estimated cost is approximately $4230, which is broken down into $920 for materials, $520 for manufacturing, and $2790 for electronics. The most expensive part is central cable motor, which costs $1000. Due to the current shortage of the supply chain and urgent timeline, we purchase the expensive motor to verify our system first. We believe we can find alternative item under $100 when system verification is done, and the overall cost will be under $1000 at the commercial manufacturing stage.

Objective#2: Manipulator integration with a low-cost machine vision system and selected end-effector tools (e.g. for picking, year 1) (Karkee – Lead, Luo – Co Lead).

Overview in the proposal: To prototype a robotic system for field testing with various operations, we will develop a perception system and integrate it with the soft, growing manipulator. In addition, a

commercially available cable driven soft gripper will be integrated (one at a time) with the end-effector mount (Obj # 1) to support apple harvesting use case.

Our current achievement:

Perception: The global ZED2 depth camera and image processing system developed can provide target apples' 3D location and the relative position of the manipulator's end-effector to build the close loop system.

Soft gripper: 0.66 lbs and can grasp an apple without the force feedback control

Objective#3: Design and implement a low-level controller to achieve automated operation (Luo – Lead).

Overview in the proposal: Once the perception/vision system, end-effector tool (Obj#2) and soft manipulator (Obj#1) have been tested separately for their functionality, they will be integrated together for overall system evaluation in the simulated, laboratory environment as well as in the field environment using automated motion/control techniques discussed below.

Our current achievement:

Our research team is working on the system integration including the robotic platform, perception, and soft robotic gripper. Currently, the robotic arm's motion can be teleoperated, and we will implement the low-level controller after the system integration. Figure. 1 summaries the goals and our current progress.

Overall progress

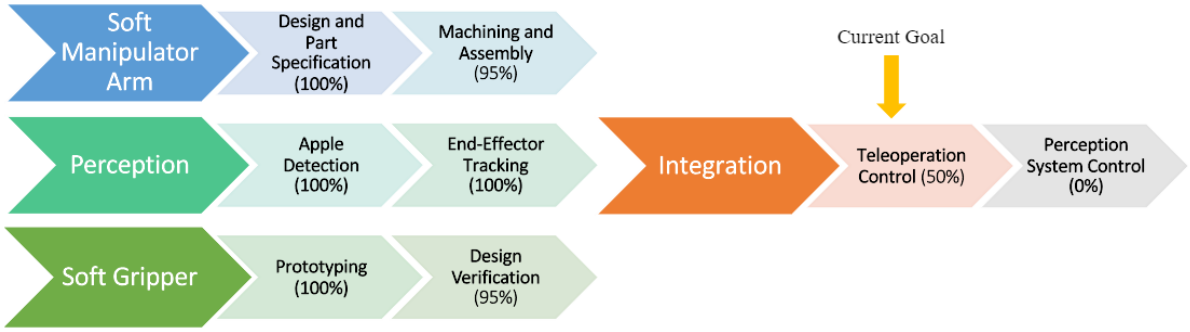

Figure. 1 Goals vs Current progress

Results and Discussion

So far, our research team have reached 90% of the overall goal with 1-year funding provided to the team in 2022. One design change we implemented was to reduce the soft-manipulator length from proposed 7-ft to 4-ft as it was found to be optimal for modern orchard architectures. Our research team is in the process of system integration, which will be completed (including the low-level control) by the end of funding period (02/2023).

Executive Summary

Project title: Low-cost, reliable soft arm for automated tree fruit operations

Keywords: Manipulator, Fruit, Harvesting

Abstract: During this one-year project, we have completed and verified all sub-components of our soft growing manipulator to achieve robotic apple harvesting with a soft manipulator: robot design and prototyping, local perception system development, and the end-effector tools. In the rest of this project period (by Feb, 2023), we will conduct the system integration and implement the low-level position control to our system.

1. Overview

Our report introduces three components: robot, perception system and the end-effector for apple harvesting. Each component includes the requirement of its functionality and our approach and experimental verification. Lastly, we will include one sub-section to discuss the cost of the technology being developed.

2. Soft Growing Manipulator

2.1 Requirement

In this project, several key design decisions were made to meet the desired specifications. In particular, these decisions revolved around the pressurized enclosure, motors, steering system, pressure control system, and fabric selection. These choices balanced the functional requirements with the cost in order to minimize cost of manufacturing while maximizing performance.

For the pressurized enclosure, the primary requirement was the maximum internal pressure for the system. The original goal for this project was a maximum internal pressure of 20 psi. Thus, the enclosure had to hold this high pressure with a factor of safety of at least 2. So, to meet this requirement, the enclosure was chosen to be made out of machined aluminum. This choice allows the enclosure to hold significantly high pressures while being easily machinable. The enclosure was also designed to use readily available stock tubes and aluminum plates. This choice decreased the overall cost and machining time.

The motors were chosen based on the torque required to get the desired motion for steering, extension and retraction. The steering motors were chosen based on a buckling test conducted on the arm whilst it was pressurized. This test involved using a force scale to pull on one of the heat-welded tabs on the tube arm to approximately 30 degrees in one direction. From preliminary testing, the force to buckle the tube at 3 psi and 10 psi was estimated to be around 15 lbs and 30 lbs respectively. With these results, the torque required to buckle the tube is only dependent on the radius of the steering pulleys. The steering pulleys have a radius of 0.5 in. Thus, the torque required to kink the tube at 3 and 10 psi is 7.5 lb*in and 15 lb*in respectively. The chosen gear motors have a torque rating of approximately 42.5 lb*in, which exceeds the minimum torque requirement. This decision was made to ensure that the steering motors could buckle the arm under any condition. The central motor was chosen based on the retraction pressure. At 3 psi, the end of the arm is under approximately 24 lbs, and based on the diameter of the central pulley, the torque required to hold the arm position is around 42.2 lb*in. Despite this being lower than the torque output of the steering motors, the steering gearmotors could not be used for this application. This is due to the slow free spin speed of the steering gearmotors. For the arm to extend at a reasonable speed without damaging the central motor, a high torque and high free spin speed gearmotor is needed.

For the rest of the steering system, various design choices were made to ensure reliability, reduce manufacturing time, and prolong fabric arm integrity. Firstly, a steering guide plate was attached to the

front of the manipulator arm base in between the steering motors and the steering collar. The guide plate directs the steering cables in the appropriate direction and orientation. This component provides a level of consistency in the assembly and control of the device. Secondly, a steering collar was designed to mount onto the fabric arm at the heat-welded tabs. This collar provides a consistent location for the steering cables to attach to the fabric arm. The collar also reduces the complexity of the fabric arm design and distributes the steering torque load on the arm. This makes manufacturing the fabric arms easier and prolongs the life of the heat-welded tabs.

For the pressure control system, a high flow rate low pressure tolerable digital pressure regulator was chosen. This was based on the intricate requirements of the system. For this system, the minimum pressure is 3 psi and the maximum pressure is 10 psi. These pressures are relatively low for pneumatic systems since typical pneumatic valves only function at around 15 psi. So, a low-pressure tolerable device is needed for this system. The system also has to be able to switch between these pressures at a fast speed. Thus, a high flow rate is required to get the system to switch as fast as possible. Based on these requirements, a digital pressure regulator that can handle vacuum pressures and has the highest possible flow rate was chosen.

The fabric was chosen based on a series of tests and the pressure requirements of the system. Various heat-weldable materials were tested at different pressures. These tests aimed to evaluate the maximum pressure the heat-welded fabric could reliably hold. From this process, a heat-weldable TPU-coated fabric was chosen based on its reliable maximum pressure around 10 psi.

2.2 Design and Fabrication

For this project, an initial prototype was designed to meet the expected outcomes outlined in the project proposal, shown in Figure 2. This design uses a pressurized enclosure, manipulator arm, and electronics subsystems. All of which have their own subcomponents and interface with each other. Specifically, the pressurized enclosure has an aluminum enclosure, central pulley assembly, central motor, and pressure regulation system. The manipulator arm has the fabric arm, steering motors, steering pulleys, steering collar, steering guide plate, and the central pulley cord. The electronics system consists of the logic and motor driver circuit board, the wire connections, and the power supplies needed for all electrical components. The manipulator arm is mounted onto the front of the pressurized enclosure and the electrics subsystem is connected to all of the various electrical hardware.

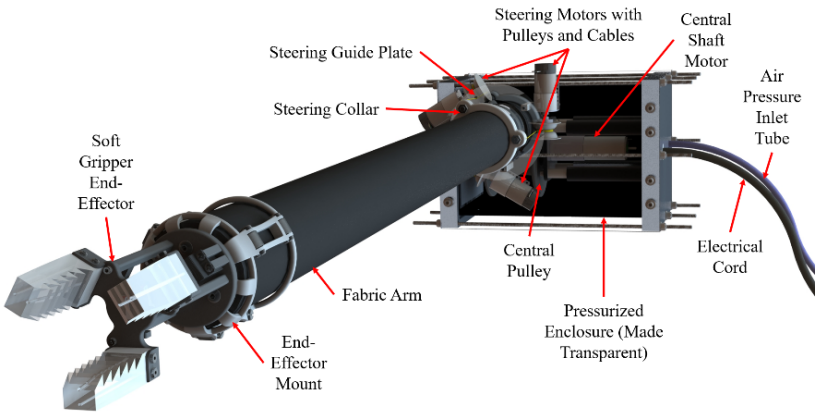

Figure. 2 Soft Growing Robotic Manipulator System

Pressurized Enclosure: The pressurized enclosure consists of an aluminum airtight enclosure that houses the central pulley assembly and central motor. The enclosure is designed to withstand high pressures while using readily available materials to reduce the overall cost. Specifically, the enclosure utilizes stock aluminum plates, a square aluminum tube, and a round aluminum tube which are easily CNCed or water-jet cut. In this design, two square aluminum plates are clamped onto the open ends of the square tube, and the round tube is threaded into a hole made in the square tube. The center of this hole is aligned to be tangent to the central pulley. There are rubber gaskets located at the interface of

the two side plates and the square tube as well as the interface of the square and round tubes. The design uses 8 threaded rods to clamp the side plates onto the ends of the square tube. Two rectangular plates mount on the front and back sides of the enclosure. The front plate provides a mounting location for the steering motors, and the back plate provides a mounting hole pattern for the entire enclosure. There are two holes in the right-side plate for the air pressure inlet and the motor power cable. The air pressure inlet uses a threaded pneumatic tube insert and the power cable is fed through a brewer's stopper to keep the system airtight. The enclosure was designed to hold up to 20 psi with a factor of safety above 2. However, the enclosure has not been tested above 20 psi due to the fabric arms rupturing at pressures below 20 psi. The maximum pressure the enclosure has been tested at so far has been 18 psi.

Central Pulley and Motor: The central motor is a 24 VDC gearmotor with a digital encoder and 1:12 gear reduction. The central motor is connected to the central pulley assembly using a modified 10mm mounting hub, and the pulley assembly is connected to the main pulley cord of the manipulator arm. The motor is mounted to the right-side plate using an aluminum mounting plate and aluminum mounting rods. The pulley assembly has a 0.5 in hexagonal shaft running through it which is supported by a 6 mm shaft that fits into a bearing mounted in the left-side plate. This configuration allows the motor to control the extension and retraction of the manipulator arm by pulling on or releasing the main pulley cord. These components are shown in Figure 3. From preliminary calculations, the free-spin speed of the central motor will allow the manipulator arm to extend at a speed of 4.8125 ft/s. However, the actual extension speed will be dependent on the extension pressure setting of the enclosure. Since the internal pressure of the arm is the driving force in the extension process. Higher internal pressure will result in a higher extension speed and vice versa. The retraction speed will be dependent on the load and the pressure setting. However, based on the rated speed of the motor, the arm will have a retraction speed of 2.292 ft/s. A large payload or higher internal pressure will reduce the retraction speed. These preliminary calculation speeds display that the design is capable of fast movement speeds. Thus, the design allows for the execution of quick movement in fruit tree operations.

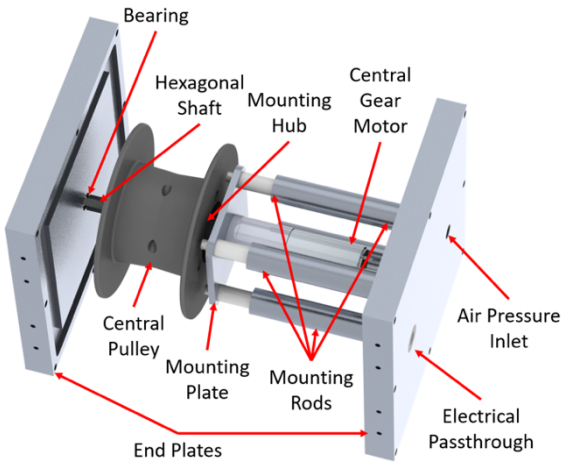

Figure. 3 Internal Components of the Pressurized Enclosure

Central Pulley Assembly: The central pulley assembly is made up of two 3D-printed PLA pulley halves, a hexagonal aluminum shaft, and a modified mounting hub. The two pulley halves are bolted together using three partially threaded bolts. There is an off-center hole at the interface of the two halves for the main pulley cord to go through and be tied off. The mounting hub is bolted to the end of the pulley using heat-inserts, and the hexagonal aluminum rod is inserted into the other end of the pulley assembly. The central pulley assembly is mounted into the pressurized enclosure by connecting one end of the aluminum rod to the central motor shaft and the other end to the bearing in the left-side plate.

Fabric Arm: The fabric arm is made from a Heat-Sealable TPU-Coated Fabric that is heat-welded together. The fabric is cut and welded into a tube-like shape with one end of the tube sealed shut. The tube has an outer diameter of 3.2 in and a length of 4.9 ft. The diameter is slightly greater than 3 in to provide enough tolerance for the inner layer of rubber used to create an airtight seal between the fabric arm and the aluminum tube. The arm length is significantly longer than 4 ft to ensure that there is enough material to seal the end and attach the arm to the enclosure. The sealed end is pulled into the body of the fabric tube and is connected to the main pulley cord. The end of the pulley cord is tied

around the sealed end of the arm. The base of the arm goes over the round aluminum tube with a sheet of rubber in between the fabric and the metal. Another sheet of rubber wraps around the fabric at the base, where two hose clamps hold the arm to the pressurized enclosure. Three TPU-coated fabric tabs are heat welded to the fabric arm at three specific points. These tabs are made out of a strip of heat-weldable fabric that was heat-welded into a 'T' shape. Then a hole is punched through the bottom part of the 'T' strip to allow the bolts in the steering collar to pass through.

Steering System: The steering system is composed of three steering motors, pulleys, cables, the steering guide plate, and the steering collar. The steering system is shown in Figure 4. This system controls the buckling or actuation angle of the fabric arm.

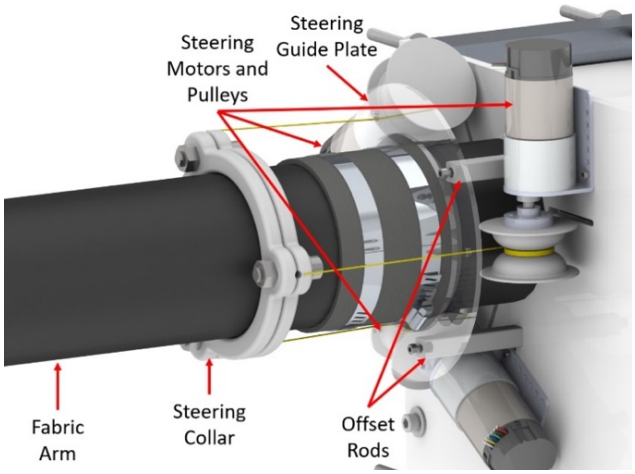

Figure. 4 Steering System Component Diagram

Steering Motors: Located at the base of the manipulator arm are three 12V DC gearmotors with digital encoders. The motors have a 150:1 gear ratio to ensure a relatively high amount of torque. The motors are fastened to mounting brackets, and these brackets are fastened to the front plate of the pressurized enclosure. The motors are connected to small pulleys, which are connected to the steering cables. The steering cables are attached to the steering collar which is mounted at the base of the fabric arm. The steering motors use the pulleys to pull at the base of the arm at specific points to buckle the base of the arm. A pressure test was conducted to determine the torque required to buckle the arm.

Steering Cables and Pulleys: The steering cables act like tendons in an arm. Specifically, they pull at the steering collar at the base of the arm at specific points and with a specified torque to kink the arm to a certain angle. The pulleys are made from 3D-printed PLA plastic and have threaded heat-inserts to fasten the pulleys to the mounting hubs on the steering motors. The pulley cords are made of a heavy-duty Kevlar braided string. This decision makes the steering pulleys and cords easily manufacturable and relatively inexpensive. The cords are tied around the bolts that clamp the steering collar together, and the cords are fed through the string openings in the steering collar.

Steering Cable Guide Plate: An acrylic plate mounted on the front of the pressurized enclosure at the base of the manipulator arm that guides the steering cables to specific angles and points on the fabric arm. The plate is made out of a 1/8-inch laser-cut acrylic sheet to decrease cost and manufacturing time. The steering cable guide plate helps provide a level of consistency in the set-up of the steering system. This consistency greatly improves the modeling and control of the system. The steering guide plate is mounted to the front mounting plate using 3D-printed PLA offset rods.

Steering Collar: The steering collar is made out of two 3D-printed PLA plastic circular plates that are clamped together using three threaded bolts with washers and nuts. The collar plate is a circular loop with an inner hole of the same diameter as the fabric arm and three tabs for the clamping bolts. The steering collar goes over the fabric arm and is mounted to the arm at a specified point by clamping the collar onto heat-welded fabric tabs on the arm. By clamping the collar onto these tabs, the collar's position on the arm is fixed. The steering cables are tied to the bolts in-between the two plates and are pulled through specially designed gaps in-between the plates. This configuration makes it so that the steering cables pull on the bolts rather than the 3D-printed plastic. The steering collar allows for distributed steering loads and easily adjustable steering mount locations. It also makes the production

of fabric arms far less time-consuming and expensive. The steering collar also dramatically reduces the impact of fatigue on any heat-welded joints.

Pressure Regulation System: The pressure regulation system consists of a single digital closed-loop pressure regulator, pneumatic tubing, a hand-adjustable pressure regulator, and a building's air supply, shown in Figure. 5. The hand-adjustable pressure regulator restricts the building air supply pressure to safe operating pressures. The digital pressure regulator controls the operating pressure of the system and is connected to the hand-adjustable pressure regulator. This process also reduces the pressure gradient required for the digital pressure regulator to control. The connections between all components are 0.5 in OD vinyl pneumatic tubing.

Figure. 5 Hand Adjustable Pressure Regulator (Left) Digital Pressure Regulator (Right)

Electronics Subsystem: The electronics are composed of a single soldered breadboard circuit board that controls the logic, motor drivers, and pressure regulator. The three steering motors all use the same model of 12V DC motor driver, while the central motor has its own 24V DC model. One 12V DC power supply and one 24 V DC power supply are used to power the entire system. The entire system is shown in Figure 6.

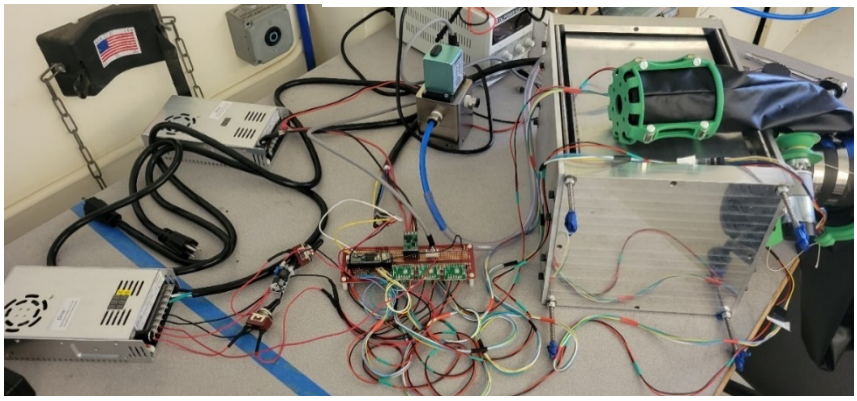

Figure. 6 Entire Electronics Subsystem of the Manipulator Arm

End-effector Mount: Located at the end of the manipulator arm is the end-effector mount, which has an internal and an external component. Shown in Figure 7. The internal component travels inside of the fabric arm while the external component travels outside of the arm. Both components are made from 3D-printed PLA plastic and are easily manufacturable. These components stay together using rolling magnets that are strong enough to hold the 3 lbs payload without disconnecting. Specifically, the end-effector mount can hold up to 6 lbs vertically before the magnets begin to slip. The external component has six mounting holes located on the front plate to allow any desired end-effector to be mounted.

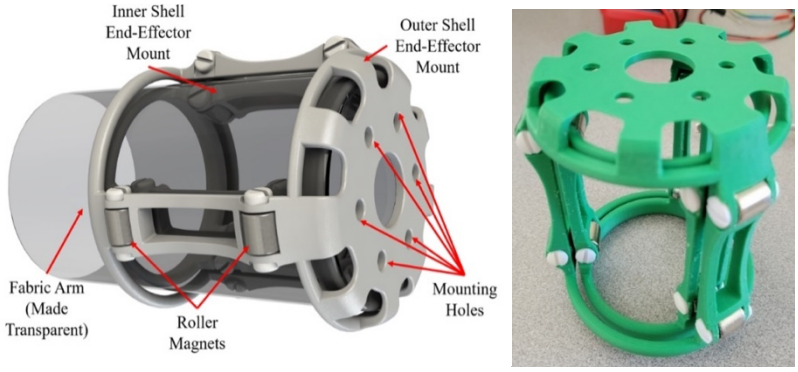

Figure. 7 Labeled Component End-Effector Mount Diagram (Left) Physical 3D Printed End-Effector Mount (Right)

2.3 Experimental Verification

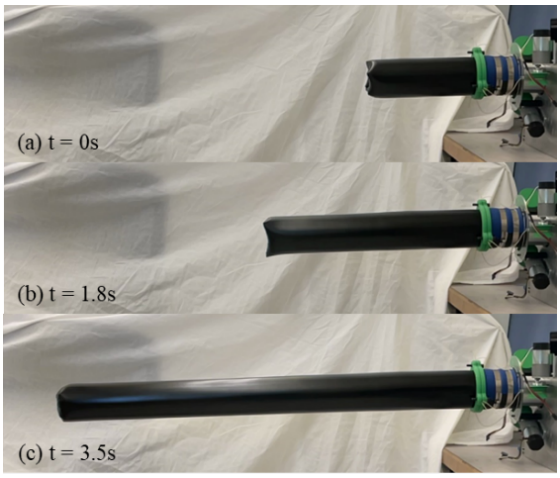

Figure. 8 Arm Extension Process (a) Initial Position at t=0s (b) Half-way position at t=1.8s (c) Full Extension at t=3.5s

Growing Speed Testing: The growing speed of the manipulator arm was determined by analyzing a slow-motion video of the arm extension process. This process involved pressurizing the arm to a predetermined pressure, then allowing the arm to extend, and then using a video analysis program to determine the speed of the extension. For this test, the arm was pressurized to 7 psi, due to lab safety concerns, higher pressures were not tested. Once the system was pressurized, the central motor was set to freely spin, allowing the arm to extend. This process is shown in Figure 8. Next, the video of this process was loaded on a computer with the software Tracker. The software tracked the position of the end of the arm over a time interval. Through this process, the extension speed of the arm was found to be 0.7 ft/s at 7 psi. However, based on calculations, the manipulator arm is capable of reaching an extension speed of 1.7 ft/s. The discrepancy between these two speed values can be attributed to the low internal pressure setting, low inlet airflow rate, and friction between sections of the arm fabric. We are working on increasing the extension speed by increasing the maximum internal pressure and airflow rate of the system.

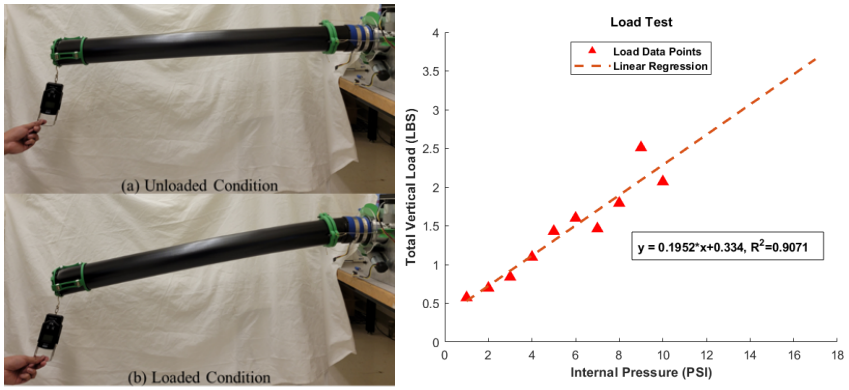

Figure. 9 Payload Testing Process (a) No Applied load (b) Applied Load Induces Buckling at the Base of the Arm (Left) Plot of the Total Vertically Applied Load, in lbs, over the Internal Pressure, in psi (Right)

Manipulator Arm Payload Testing: The maximum payload of the manipulator arm was determined by conducting a simple load test. This process involved pressurizing the system to a set pressure and then pulling the end of the arm down with a digital force scale until the base of the arm buckled and the robot loses control. This process is shown in Figure 9. The force measurement reading from the scale was then recorded. This process was repeated three times for a given pressure reading and then the entire measurement process was repeated for pressures ranging from 1 to 10 psi in 1 psi increments. The average of the three data points for each pressure was taken to account for irregularities. This data was then loaded into Microsoft Excel, where a linear regression was performed to estimate the maximum load of the manipulator arm at higher pressures. Based on fabric arm pressure tests, we set the safe operating pressure range to pressures below 15 psi. Thus, due to lab safety concerns, we only tested the arm once at 9 and 10 psi. We are working with a polymeric fabric expert to increase the maximum safe operating pressure of the fabric arms. The results of this process are shown in Figure 8. This plot shows that the manipulator arm is capable of supporting a 2 lbs payload at approximately 9 psi. This payload is more than sufficient to hold the end-effector and carry a large apple.

Workspace and Steering Testing: To determine and verify the workspace of the manipulator arm, the physical limitations of the system were used. These physical limitations include the maximum actuation angle of the arm in a 2D plane and the maximum length of the arm. From preliminary testing, the maximum actuation angle of the arm was found to be 30 degrees from the neutral position. This actuation angle is shown in Figure 10. Since this result was from a single motor actuating in a single direction, the total maximum actuation angle for the manipulator arm is 60 degrees in the 2D plane. The maximum length of the arm, of 4 ft, was predetermined during the manufacturing of the arm. With this information, the workspace of the manipulator arm was determined to be a spherical sector with a radius equal to the maximum arm length and 60 degrees of actuation in the 2D plane. This workspace is shown in Figure 11. This workspace was verified by a simple movement test, in which the arm length and actuation angle of the arm were adjusted. Next, the workspace of the manipulator arm was compared to the camera view, shown in Figure 11. From this process, the 6*6-ft and 3 ft depth camera view was found to match the workspace of the manipulator arm very well.

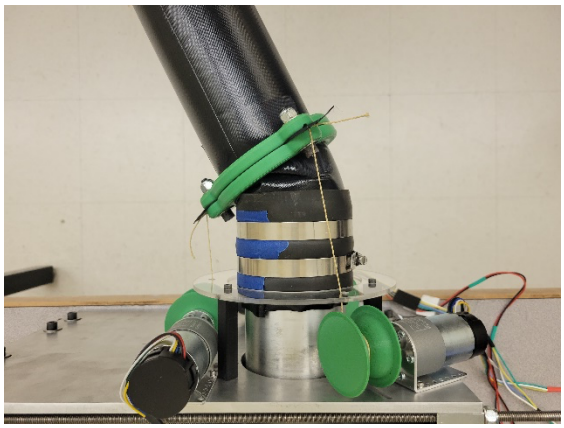

Figure. 10 Manipulator Arm Steering Test

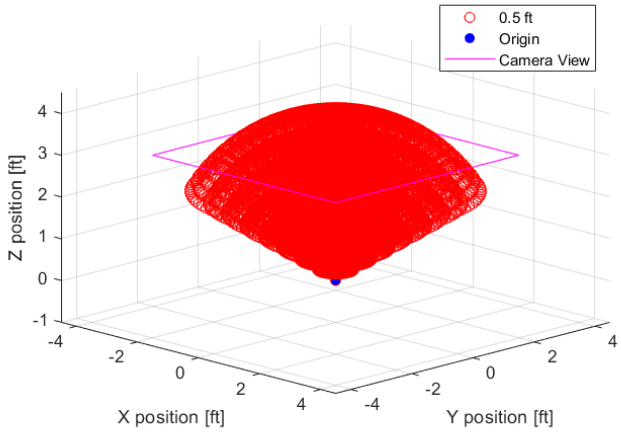

Figure. 11 Plot of the Manipulator Arm Workspace and the Camera View

3. Perception

3.1 Requirement

The perception system includes two subsystems: i) apple detection system; and ii) end-effector tracking systems with one single ZED 2 depth camera. The apple detection system is based on the modified You-Only-Look-Once (YOLO) v5 model to detect the mature apples on the apple canopy in the field environment. Since there is no attitude sensing for the soft manipulator, it is necessary to provide a vision system solution that tracks the pose of the end-effector to achieve a close-loop control system to achieve precise apple harvesting.

3.2 Components

Figure. 12 Apple detection training images for YOLv5s

Apple detection system: The apple detection system was specialized for the vertical fruiting-wall tree architecture, as a common SNAP (simple, narrow, accessible, and productive) system planted in WA (experimental orchard was located in Prosser, WA). A database including 1,600

RGB images collected by Co-PI Karkee's team from the 2017 and 2018 harvesting seasons was used as a training dataset in this research (Figure 11). There were around 10~20% of the apples from the background, which were not suitable harvesting targets. A total of 800 images in the dataset were applied with a depth filter to remove the background, including unwanted apples from the adjacent rows. All images were annotated manually with rectangular annotations of the 'apple' class and corresponding annotation files were saved. The dataset was used as an input for training a modified YOLOv5s [1].

End effector detection system: To track the 3D location and orientation (attitude) of the end-effector in the global camera's frame, we adopted the "ArUco Marker tracking" method [2]. ArUco markers are binary square markers that can be used for camera pose estimation (shown in Figure 13). We attached a 2*2*2-in lightweight cube with six different ArUco codes (one in each face of of the cube) to the end effector (Figure 13). These codes were detected to estimate 6 DoFs (location and orientation in 3D) of the end-effector in real-time. The mechanism of this algorithm is that the 6 DoFs information can be calculated if two different ArUco markers of the cube can be detected by a single camera. The benefit of this algorithm is that this approach is robust, fast and simple (binary detection without dealing color information).

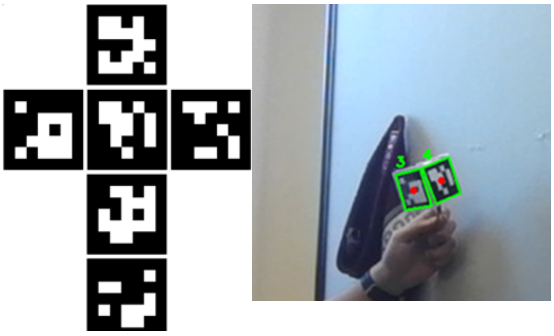

Figure. 13 ArUco Codes Print-Out (Left) and ArUco Cube track the end effector (Right)

3.3 Experimental results.

Apple detection system: The apple detection system was built on a modified YOLOv5s with backbone (GhostNet) and neck (Bi-FPN). The mean average precision of the proposed model in this project was 95.4% based on a testing dataset including 100 images. The average processing speed was 43.5 frames per second (22 ms per image) with an image resolution of 648*648 pixels. The detection results indicated that the vision system achieved good performance in open-field environments while keeping a real-time detection speed. The effective range of apple detection was between 1.3 and 7.5 ft. An example output of the apple detection system is shown in Figure 14. The image processing system faced some challenges with occlusion of apples from the canopy objects.

Figure. 14 Apple detection in orchard environment

End effector detection system: As discussed above, the ArUco code cube was attached to the top of the end-effector, which could show at least one surface to the camera during the movement of the manipulator. The processing speed on ArUco cube detection and pose estimation was 32.5 frames per second, which is sufficient for the low-level position control developed in this work.

Integrated Vision/Perception System: Figure 15 shows the overall perception process. A ZED 2 camera, located on the top of the robotic arm's container, provided one stationary 2D image with depth information. Image processing technique estimated 3D location of target apples and end-effector, which will be sent to the planner to generate the optimal sequence that the single robotic manipulator should follow (will develop the optimal planning algorithm with the next year's funding). In the future orchard evaluation, we may adapt two ZED 2 cameras to deal with more unpredictable environments with the same algorithms to detect target apples and the end-effector.

Figure. 15 One ZED 2 camera provided 3D position of target apples and 6 DoF (position and orientation) of the end- effector in global camera frame.

4. Soft Robotic Gripper

4.1 Requirement

For the soft gripper end-effector, a lightweight, highly supportive, and low-impact end-effector was needed. Specifically, the gripper could not weigh more than 0.66 lbs, the gripper had to hold large apples weighing up to 0.66 lbs without slipping, and the gripper could not damage the fruit during picking. To accomplish these objectives several key design decisions were made. Firstly, the frame and palm of the gripper were made out of 3D-printed PLA plastic. This allowed for lightweight rapid prototyping and design testing. Secondly, a servo-actuated pulley system was used to contract the gripper fingers around the target apple. This system used a cable actuation method whereby one side of the finger is contracted while the other is released. A pulley system is simple, lightweight, and can induce the torque needed to contract the fingers of the gripper. This system also allows the gripper fingers to wrap around the target apple, restricting its movements while giving sufficient support. The servo is also relatively inexpensive and has moderate weight for its size. Thirdly, the gripper fingers were chosen to be made out of DragonSkin30 silicon rubber. This silicon rubber has a high stiffness but is still soft to the touch. Thus, it easily supports the weight of the apple without causing any damage to the fruit. This silicon rubber is also relatively lightweight and has moderate friction with apple skin. Fourthly, the palm of the gripper was made out of 3D-printed PLA and was made with a 1.15 in radius. This kept the design lightweight, increased the potential amount of surface area the fingers could grab onto the apple, and reduced the likelihood of an apple slipping between the fingers. Lastly, a limit switch was used as the activation method for the gripper. The simplicity of this method reduced the weight and complexity of the overall design.

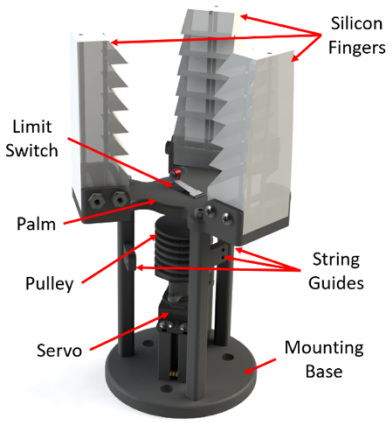

Figure. 16 Components of the Soft Gripper End-Effector

4.2 Design and Fabrication

Soft Gripper Frame and Palm: All structural components of the soft gripper end-effector are made out of 3D-printed PLA plastic. This allowed for rapid prototyping and testing while minimizing overall weight. The structural components include the mounting base, string guide support rods, the palm,

servo mounting rods, and the pulley. The mounting base can be connected to the end-effector mount at the end of the manipulator arm. The support rods and the servo mounting rods are bolted directly to the mounting base. The support rods have guide holes for the strings on the pulley at certain levels to ensure the strings are guided properly. The pulley is attached to a servo motor, and the palm is bolted to the support rods. The limit switch is fitted into a hole in the palm and the silicon fingers are bolted to the mounting locations in the palm. This design is shown and labeled in Figure 16.

Silicon Fingers: The fingers of the soft gripper end-effector are made out of DragonSkin30, a high-stiffness silicon rubber. From preliminary testing, the fingers require a high multidirectional stiffness in order to properly support the weight of the apple and resist the opposing forces during apple picking. The fingers were made using a 3D-printed PLA plastic mold and rod inserts to create the mounting holes and thread holes. Due to the wear caused by the internal threads, M2 nuts were embedded into the silicon rubber during the molding process. These nuts act as bearings inside the silicon, limiting the damage caused by wear, and thereby prolonging the life of the fingers.

Pulley System: The pulley system is composed of the servo motor, the 3D-printed pulley, and the strings threaded through the silicon fingers. The servo and the pulley were mounted vertically to reduce weight and the complexity of the design. The strings on the pulley alternate in winding so that when the pulley rotates one set of strings release off the pulley while the other set is pulled onto the pulley. This allows for the pulley system to contract one side of the fingers while releasing the other side of the fingers. The strings are threaded through the string guides on the supporting rods and then threaded through the silicon fingers. At the top of each finger, the threads are crimped together using aluminum metal crimps and then hot-glued to ensure that the tension in the threads does not loosen.

4.3 Experimental Verification

Apple Picking Test: To verify the design and functionality of the soft gripper end-effector, two prototypes were tested at two different apple orchards. One was tested in Prosser on Dave Allen's commercial apple orchards, and the other in Pullman on the Spillman Farm's traditional apple orchards. We realize that apples vary widely between different varieties and farming styles. Prosser utilizes modern trees which are easier to pick while Pullman utilizes traditional trees which are more challenging to pick. However, successfully picking an apple, in either case, verifies the functionality of the design. The first prototype was tested in the Prosser orchard but could not reliably pick apples. This was due to multiple key design flaws that were remedied in the second prototype. This new prototype was tested in the Pullam orchard during inclement weather. During this, the gripper was able to successfully pick multiple apples. The process of a successful apple pick is shown in Figure 17. While this design was successful under poor weather conditions, we are still working on improving this design. For example, we are working on making the design more adaptable for various apple sizes. This involves allowing for adjustable palm size, controllable finger gaps, and adjustable string tensioning. We are also looking into increasing the friction between the fingers and the apple surface so that the gripper will more reliably hold onto an apple even in inclement weather.

Figure. 17 Successful Apple Picking Process (a) Gripper Approaches Apple (b) Finger Contract around Apple (c) Gripper Pulls Away with Apple in its Grasp

5. Overall R&D cost of a single robotic arm

In total, the materials including 3D printing, store bought components, and stock metal for this project cost approximately $920, the manufacturing cost (CNCing, water-jet cutting, and milling cost) was $520, and the electronics cost was $2790. Specifically, the stock metal cost was $405, the ZED 2 Stereo Camera cost was $449, the gearmotors cost was $1046. Thus, the R&D cost for the entire manipulator is approximately $4230, which is about 8 times cheaper than a typical 6 degree of freedom robotic arm. Since this is rapid prototyping that needs to verify our proposed solution and the current pandemic causes the shortage supply chain issue, some components' functionalities much beyond our system's specification. For example, we purchase an approximately $1000 Maxon motor to control the robotic length, and this can be replaced by much cheaper brushless DC motor. Before the commercialization, customized circuit board including controllers and drivers and the supply chain for those motors needs to be worked more, which beyond this R&D project. PI Luo has much experiences on the technology transfer (Dr. Luo helped two technology patents be commercialized before). The cost of an entire manipulator should be around $1000 without camera system when at the manufacturing stage.

Reference:

1. Prokscha, R., M. Schneider, and A. Höß, Efficient Edge Deployment Demonstrated on YOLOv5 and Coral Edge TPU.
2. Sani, M.F. and G. Karimian. Automatic navigation and landing of an indoor AR. drone quadrotor using ArUco marker and inertial sensors. in 2017 international conference on computer and drone applications (IConDA). 2017. IEEE.